Running coupling in nonperturbative QCD: Bare vertices and y-max approximation

D. Atkinson* and J. C. R. Bloch†
Institute for Theoretical Physics, University of Groningen, Nijenborgh 4, NL-9747 AG Groningen, The Netherlands
(Received 7 January 1998; published 7 October 1998)

A recent claim that in quantum chromodynamics (in the Landau gauge) the gluon propagator vanishes in the infrared limit, while the ghost propagator is more singular than a simple pole, is investigated analytically and numerically. This picture is shown to be supported even at the level in which the vertices in the Dyson-Schwinger equations are taken to be bare. The gauge invariant running coupling is shown to be uniquely determined by the equations and to have a large finite infrared limit. [S0556-2821(98)04421-X]

PACS number(s): 12.38.Aw, 11.10.Gh, 12.38.Lg

I. INTRODUCTION

The proof of the renormalizability of non-Abelian gauge theories such as QCD [1], and the discovery of ultraviolet asymptotic freedom [2], heralded a new phase in the acceptance of quantum field theories as serious candidates for the quantitative description of the weak, electromagnetic and strong interactions. Since the running coupling in QCD decreases logarithmically to zero as the renormalization point is taken to infinity, it seems reasonable to calculate it perturbatively in the deep ultraviolet regime, where it is very small, even though a proof is lacking that the perturbation series makes sense (for example, that it is strongly asymptotic).

Although one is not sure that perturbation theory is reliable for QCD at very high energies, at very low energies it is quite clear that it is inadequate. Chiral symmetry breaking and fermion mass generation are typically non-perturbative phenomena. The obverse of ultraviolet asymptotic freedom is infrared slavery or confinement. Since the coupling decreases as the energy increases, it increases as one goes to lower energies, and the possibility is open that its infrared limit is infinite. Many attempts [3]—necessarily of a non-perturbative nature—have been made to show this divergence of the coupling in the infrared limit. Mandelstam initiated the study of the gluon Dyson-Schwinger equation in the Landau gauge [4]. Although he did consider the gluon-ghost coupling, Mandelstam concluded provisionally that its effect could safely be neglected. This assumption was also made in subsequent work [5,6]. A deficiency of these attempts to show that the gluon propagator is highly singular in the infrared is the necessity to posit certain cancellations of leading terms in the equations. An uncharitable case of *petitio principii* might almost be made (i.e. circularity).

Recently, a new possibility has been opened up by the work of von Smekal, Hauck and Alkofer [7]. In this work the coupling of the gluon to the ghost was not neglected. These authors claim that it is not the gluon, but rather the ghost propagator that is highly singular in the infrared limit. The running coupling itself has a *finite* though quite large value in the limit of zero energy, presumably large enough to guarantee chiral symmetry breaking in the quark equation [8].

In the present paper we investigate the claims made in the new work. We shall write the gluon propagator in Landau gauge as

$$D^{ab}_{\mu\nu}(p) = -\delta^{ab}\frac{1}{p^2}\Delta_{\mu\nu}(p)F(-p^2),$$

where a and b are color indices, and where $\Delta = \Delta^2$ is the projection operator

$$\Delta_{\mu\nu}(p) = g_{\mu\nu} - \frac{p_\mu p_\nu}{p^2}.$$

The ghost propagator will be written in the form

$$G^{ab}(p) = -\delta^{ab}\frac{1}{p^2}G(-p^2),$$

and we shall refer to the scalar functions F and G as the gluon and ghost form factors, respectively.

The claim made in Ref. [7] is that, in the infrared limit $x = -p^2 \to 0$, these form factors have the following behavior:

$$F(x) \sim x^{2\kappa}, \quad G(x) \sim x^{-\kappa}, \tag{1}$$

where $\kappa \approx 0.92$. To obtain these results certain *Ansätze* were made for the three-gluon and ghost-gluon vertices, functional forms inspired, but not uniquely determined by Slavnov-Taylor identities. In fact the *Ansatz* made in Ref. [7] for the ghost-gluon vertex is such that actually the infrared behavior Eq. (1) is not consistent with the Dyson-Schwinger equations. The difficulty is the occurrence of a term

$$\int_0^{\Lambda^2} dyy \int_0^{\pi} d\theta \, \frac{\sin^4\theta}{z^2} \, \frac{F(z)G(z)G(y)}{G(x)} \tag{2}$$

in the equation for the ghost form factor, which, with the form (1), would yield an impermissible $\log x$ factor in the limit $x \to 0$ when the angular integrals are performed exactly, as shown in Appendix A. The $\log x$ problem persists if one adopts the simple y-max angular averaging. Von Smekal *et al.* introduce a modified angular averaging, after which the $\log x$ problem disappears; but since their equations do not have a solution of the form (1) *before* averaging, it would seem that the averaging is not justified—it completely

*Email address: atkinson@phys.rug.nl
†Email address: bloch@phys.rug.nl

changes the properties of the equation.

Since we found this last replacement questionable, we decided first to see what would happen if one simply replaces the full vertices by bare ones. In this case the problematic logarithm of Eq. (2) does not occur, and we can simply analyze the equation as it stands. If the behavior (1) were to go away, it would bode ill for the new approach. However, our finding is that, with bare vertices, the form (1) indeed remains good, but with the index changed to $\kappa \approx 0.77$. Moreover, we can show that the solutions of the coupled gluon and ghost equations lie on a three-dimensional manifold, i.e. the general solution has three free parameters; nevertheless all solutions have the infrared behavior (1). Our primary purpose in this initial paper is to explain the above findings in detail.

In Landau gauge, the QCD Dyson-Schwinger equations lead to the following coupled integral equations for the renormalized gluon and ghost form factors:

$$F^{-1}(p^2) = Z_3 + \frac{g^2}{8\pi^3}\tilde{Z}_1 \int_0^{\Lambda^2} \frac{dq^2}{p^2} G(q^2) \times \int_0^{\pi} d\theta \, \sin^2\theta M(p^2,q^2,r^2) G(r^2) + \frac{g^2}{16\pi^3} Z_1 \int_0^{\Lambda^2} \frac{dq^2}{p^2} F(q^2) \times \int_0^{\pi} d\theta \, \sin^2\theta Q(p^2,q^2,r^2) F(r^2) \tag{3}$$

$$G^{-1}(p^2) = \tilde{Z}_3 - \frac{3g^2}{8\pi^3}\tilde{Z}_1 \int_0^{\Lambda^2} dq^2 q^2 G(q^2) \times \int_0^{\pi} d\theta \, \frac{\sin^4\theta}{r^4} F(r^2), \tag{4}$$

with $r^2 = p^2 + q^2 - 2pq\cos\theta$. The kernels are

$$M(p^2,q^2,r^2) = \frac{1}{r^2}\left(\frac{p^2+q^2}{2} - \frac{q^4}{p^2}\right) + \frac{1}{2} + \frac{2q^2}{p^2} - \frac{r^2}{p^2}.$$

$$Q(p^2,q^2,r^2) = \left(\frac{p^6}{4q^2} + 2p^4 - \frac{15q^2p^2}{4} + \frac{q^4}{2} + \frac{q^6}{p^2}\right)\frac{1}{r^4} + \left(\frac{2p^4}{q^2} - \frac{19p^2}{2} - \frac{13q^2}{2} + \frac{8q^4}{p^2}\right)\frac{1}{r^2} - \left(\frac{15p^2}{4q^2} + \frac{13}{2} + \frac{18q^2}{p^2}\right) + \left(\frac{1}{2q^2} + \frac{8}{p^2}\right)r^2 + \frac{r^4}{p^2q^2}.$$

Here the full three-gluon and the ghost-gluon vertices have been replaced by their bare values, while the four-gluon and quark-gluon vertices have been provisionally thrown away. To obtain these equations from the Dyson-Schwinger equations, we performed a contraction with the tensor $(g_{\mu\nu} - 4p_\mu p_\nu/p^2)$, introduced by Brown and Pennington [6] to avoid quadratic ultraviolet divergences, executed a Wick rotation, and evaluated two trivial angular integrations.

The form factors and the QCD coupling are renormalized at a scale μ, using the renormalization constants $Z_3, \tilde{Z}_3, Z_1, \tilde{Z}_1$ for the gluon field, the ghost field, the triple gluon vertex and the gluon-ghost vertex defined by

$$\bar{F}(p^2,\Lambda,\xi) = Z_3(\mu,\Lambda,\xi) F(p^2,\mu,\xi),$$

$$\bar{G}(p^2,\Lambda,\xi) = \tilde{Z}_3(\mu,\Lambda,\xi) G(p^2,\mu,\xi), \tag{5}$$

$$g = \frac{Z_3^{3/2}(\mu,\Lambda,\xi)}{Z_1(\mu,\Lambda,\xi)} g_0 = \frac{\sqrt{Z_3(\mu,\Lambda,\xi)}\tilde{Z}_3(\mu,\Lambda,\xi)}{\tilde{Z}_1(\mu,\Lambda,\xi)} g_0, \tag{6}$$

where $\bar{F}(p^2), \bar{G}(p^2)$ are the unrenormalized gluon and ghost form factors, $F(p^2), G(p^2)$ the renormalized ones, g_0 is the bare coupling and g its renormalized value. We will see in the following sections that the concept of renormalization scale can be generalized in the nonperturbative treatment to what we will call renormalization prescriptions, each corresponding to a solution of the nonperturbative integral equations. The renormalization group invariance of the running coupling corresponds to an invariance under an arbitrary transformation in the three-dimensional space of solutions of the integral equations.

We wish to solve the coupled integral equations (3), (4) for F and G, and we propose to do that in a future publication [9,10]. For the moment we introduce a further simplification, the y-max approximation. This amounts to replacing $F(r^2)$ and $G(r^2)$ in Eqs. (3), (4) by $F(p^2)$ and $G(p^2)$ if $p^2 > q^2$, but by $F(q^2)$ and $G(q^2)$ if $p^2 \leqslant q^2$. This approximation facilitates the analytical and numerical analysis of the equations, since the angular integrals can now be performed exactly, and indeed the resulting one-dimensional Volterra equations can be converted into nonlinear ordinary differential equations. This y-max approximation is very widely employed for these reasons, however let us sound a note of warning: although we do not expect the qualitative picture of the solutions (1) to change, we do expect the value of the index κ to be different when we treat the coupled equations without the y-max approximation [9]. We have already seen that κ is sensitive to the choice of *Ansatz* for the vertex functions, and it is also affected by the y-max approximation. The bare vertex *Ansatz* is of course only a first guess; and it is clear also that the *Ansatz* of von Smekal *et al.* needs to be improved to avoid the logarithm problem to which we alluded above. Nevertheless, the picture that von Smekal, Hauck and Alkofer have uncovered appears to be robust in its qualitative, and hopefully also in its semi-quantitative features: the gluon propagator is *soft* in the infrared (i.e. it vanishes in this limit, instead of blowing up like a pole), while

the ghost propagator is *hard* (it is more singular than a pole). The consequences for the physics of the strong interaction need to be investigated.

II. THE COUPLED GLUON-GHOST EQUATIONS

The set of coupled integral equations for the gluon and ghost propagator, using the bare triple gluon vertex and the bare gluon-ghost vertex, and introducing the y-max approximation in Eqs. (3), (4), is as follows:

$$F^{-1}(x)=Z_3+\lambda\tilde{Z}_1\Bigg[G(x)\int_0^x\frac{dy}{x}\left(-\frac{y^2}{x^2}+\frac{3y}{2x}\right)G(y)+\int_x^{\Lambda^2}\frac{dy}{2y}G^2(y)\Bigg]+\lambda Z_1\Bigg[F(x)\times\int_0^x\frac{dy}{x}\left(\frac{7y^2}{2x^2}-\frac{17y}{2x}-\frac{9}{8}\right)F(y)+\int_x^{\Lambda^2}\frac{dy}{y}\left(-7+\frac{7x}{8y}\right)F^2(y)\Bigg] \tag{7}$$

$$G^{-1}(x)=\tilde{Z}_3-\frac{9}{4}\lambda\tilde{Z}_1\Bigg[F(x)\int_0^x\frac{dy}{x}\frac{y}{x}G(y)+\int_x^{\Lambda^2}\frac{dy}{y}F(y)G(y)\Bigg], \tag{8}$$

where $\lambda=g^2/16\pi^2$, $x=p^2$ and $y=q^2$.

To solve Eqs. (7), (8), we eliminate the renormalization constants Z_3 and $\tilde{Z}_3$ by subtracting the equations at $x=\sigma$:

$$F^{-1}(x)=F^{-1}(\sigma)+\lambda Z_1\Bigg[F(x)\int_0^x\frac{dy}{x}\left(\frac{7y^2}{2x^2}-\frac{17y}{2x}-\frac{9}{8}\right)F(y)-F(\sigma)\int_0^\sigma\frac{dy}{\sigma}\left(\frac{7y^2}{2\sigma^2}-\frac{17y}{2\sigma}-\frac{9}{8}\right)F(y)-7\int_x^\sigma\frac{dy}{y}F^2(y)+\int_x^{\Lambda^2}\frac{dy}{y}\left(\frac{7x}{8y}\right)F^2(y)-\int_\sigma^{\Lambda^2}\frac{dy}{y}\left(\frac{7\sigma}{8y}\right)F^2(y)\Bigg]+\lambda\tilde{Z}_1\Bigg[G(x)\int_0^x\frac{dy}{x}\times\left(-\frac{y^2}{x^2}+\frac{3y}{2x}\right)G(y)-G(\sigma)\int_0^\sigma\frac{dy}{\sigma}\times\left(-\frac{y^2}{\sigma^2}+\frac{3y}{2\sigma}\right)G(y)+\int_x^\sigma\frac{dy}{2y}G^2(y)\Bigg] \tag{9}$$

$$G^{-1}(x)=G^{-1}(\sigma)-\frac{9}{4}\lambda\tilde{Z}_1\Bigg[F(x)\int_0^x\frac{dy}{x}\frac{y}{x}G(y)-F(\sigma)\int_0^\sigma\frac{dy}{\sigma}\frac{y}{\sigma}G(y)+\int_x^\sigma\frac{dy}{y}F(y)G(y)\Bigg]. \tag{10}$$

III. SYMMETRIES OF THE REDUCED EQUATIONS

A very interesting simplification of Eqs. (9), (10) is obtained if we throw away the gluon loop in Eq. (9), keeping only the ghost loop. This truncation is particularly intriguing because, as we will show, its properties agree with the requirements of renormalization group invariance, thus allowing us to specify the running coupling in a unique way, whereas the inclusion of the approximate gluon loop introduces an ambiguity. The truncated set of equations is

$$F^{-1}(x)=F^{-1}(\sigma)+\lambda\tilde{Z}_1\Bigg[G(x)\int_0^x\frac{dy}{x}\left(-\frac{y^2}{x^2}+\frac{3y}{2x}\right)G(y)-G(\sigma)\int_0^\sigma\frac{dy}{\sigma}\left(-\frac{y^2}{\sigma^2}+\frac{3y}{2\sigma}\right)G(y)+\int_x^\sigma\frac{dy}{2y}G^2(y)\Bigg] \tag{11}$$

$$G^{-1}(x)=G^{-1}(\sigma)-\frac{9}{4}\lambda\tilde{Z}_1\Bigg[F(x)\int_0^x\frac{dy}{x}\frac{y}{x}G(y)-F(\sigma)\int_0^\sigma\frac{dy}{\sigma}\frac{y}{\sigma}G(y)+\int_x^\sigma\frac{dy}{y}F(y)G(y)\Bigg]. \tag{12}$$

We will show that Eqs. (11), (12) have a three-dimensional space of solutions and that these solutions can be transformed into one another by means of simple scalings.

First of all, if we have a solution $F(x)$ and $G(x)$, we can build a two-dimensional infinity of solutions simply by scaling these functions:

$$\tilde{F}(x)=F(x)/a \tag{13}$$

$$\tilde{G}(x)=G(x)/b \tag{14}$$

which simply amounts to a redefinition of Z_3 and $\tilde{Z}_3$, i.e. to a change in the renormalization prescription. The new functions satisfy the same integral equations, with the rescaled coupling constant:

$$\tilde{\lambda}=\lambda ab^2.$$

Although the value of λ is in general changed, this has no physical consequence, since the following gauge invariant quantity

$$\lambda F(x)G^2(x)=\tilde{\lambda}\tilde{F}(x)\tilde{G}^2(x),$$

which will be shown to be the running coupling in Sec. IV, is unchanged by the above transformations. Thus the two-dimensional manifold of solutions corresponds to the same physics.

A second, less trivial feature is the possibility to derive an infinite number of solutions starting from $F(x)$ and $G(x)$

just by scaling the momentum x to tx. The new functions $\hat{F}$ and $\hat{G}$ take the same values at momentum x as F and G at momentum tx:

$$\hat{F}(x) \equiv F(tx), \quad \hat{G}(x) \equiv G(tx). \tag{15}$$

In terms of the scaled quantities,

$$\tilde{x} = x/t, \quad \tilde{y} = y/t, \quad \tilde{\sigma} = \sigma/t$$

we find

$$\hat{F}^{-1}(\tilde{x}) = \hat{F}^{-1}(\tilde{\sigma}) + \lambda \tilde{Z}_1 \Bigg[\hat{G}(\tilde{x}) \int_0^{\tilde{x}} \frac{d\tilde{y}}{\tilde{x}} \left(-\frac{\tilde{y}^2}{\tilde{x}^2} + \frac{3\tilde{y}}{2\tilde{x}} \right) \hat{G}(\tilde{y}) - \hat{G}(\tilde{\sigma}) \int_0^{\tilde{\sigma}} \frac{d\tilde{y}}{\tilde{\sigma}} \left(-\frac{\tilde{y}^2}{\tilde{\sigma}^2} + \frac{3\tilde{y}}{2\tilde{\sigma}} \right) \hat{G}(\tilde{y}) + \int_{\tilde{x}}^{\tilde{\sigma}} \frac{d\tilde{y}}{2\tilde{y}} \hat{G}^2(\tilde{y}) \Bigg]$$

$$\hat{G}^{-1}(\tilde{x}) = \hat{G}^{-1}(\tilde{\sigma}) - \frac{9}{4} \lambda \tilde{Z}_1 \Bigg[\hat{F}(x) \int_0^{\tilde{x}} \frac{d\tilde{y}}{\tilde{x}} \frac{\tilde{y}}{\tilde{x}} \hat{G}(\tilde{y}) - \hat{F}(\tilde{\sigma}) \int_0^{\tilde{\sigma}} \frac{d\tilde{y}}{\tilde{\sigma}} \frac{\tilde{y}}{\tilde{\sigma}} \hat{G}(\tilde{y}) + \int_{\tilde{x}}^{\tilde{\sigma}} \frac{d\tilde{y}}{\tilde{y}} \hat{F}(\tilde{y}) \hat{G}(\tilde{y}) \Bigg].$$

This means that $\hat{F}(x)$ and $\hat{G}(x)$ are also solutions of the integral equations solved by $F(x)$ and $G(x)$. Again, all the solutions obtained by varying the scaling factor t correspond to the same physical picture, since a scaling of momentum merely corresponds to choosing the units for the momentum variable when renormalizing the coupling constant at a certain physical scale. It is clear that the three above-mentioned scaling properties allow us to construct the whole three-dimensional space of solutions starting from one specific solution.

IV. THE RUNNING COUPLING

This three-fold scaling invariance is important as it is connected to the renormalization group invariance of the running coupling, as we will now show.

The Green's functions are functions of momentum and in quantum field theory they are generally divergent. To render all the Green's functions finite it suffices to renormalize the parameters occurring in the original Lagrangian of the theory. The concept of multiplicative renormalizability relates the renormalized parameters to the bare parameters in a way that leaves the form of the Lagrangian unchanged. In this way a renormalized coupling is introduced. In QCD the renormalized coupling obeys the following equations:

$$\alpha(\mu) = \frac{Z_3(\mu,\Lambda,\xi)\tilde{Z}_3^2(\mu,\Lambda,\xi)}{\tilde{Z}_1^2(\mu,\Lambda,\xi)} \alpha_0 = \frac{Z_3^3(\mu,\Lambda,\xi)}{Z_1^2(\mu,\Lambda,\xi)} \alpha_0, \tag{16}$$

where $\alpha_0 = g_0^2/4\pi$ and we denote the explicit dependence of the renormalization constants on the renormalization scale μ, the ultraviolet cutoff Λ and the gauge parameter ξ. The renormalization scale μ is defined as the momentum scale where the full propagators and vertices are taken to be identical to their bare quantities, such that the renormalized form factors satisfy:

$$F(\mu,\mu,\xi) = 1 = G(\mu,\mu,\xi). \tag{17}$$

Such a renormalization is achieved by a proper choice of the renormalization constants Z_3 and $\tilde{Z}_3$ in the construction of the renormalized form functions from the unrenormalized ones, as given in Eq. (5).

From Eq. (16) and the definitions (5) of Z_3 and $\tilde{Z}_3$ we can derive the two following quantities, which are renormalization group invariants, since the right-hand sides of their definitions only involve unrenormalized quantities:

$$\tilde{Z}_1^2(\mu,\Lambda,\xi)\alpha(\mu)F(x,\mu,\xi)G^2(x,\mu,\xi) = \alpha_0 \overline{F}(x,\Lambda,\xi)\overline{G}^2(x,\Lambda,\xi) \tag{18}$$

and

$$Z_1^2(\mu,\Lambda,\xi)\alpha(\mu)F^3(x,\mu,\xi) = \alpha_0 \overline{F^3}(x,\Lambda,\xi), \tag{19}$$

where μ is the renormalization scale and x is an arbitrary momentum.

We now evaluate the renormalization group invariant expression Eq. (18) at momentum x, using two different renormalization scales x and μ and Eq. (17) (which is valid for any μ):

$$\alpha(x) = \frac{\tilde{Z}_1^2(\mu,\Lambda,\xi)}{\tilde{Z}_1^2(x,\Lambda,\xi)} \alpha(\mu)F(x,\mu,\xi)G^2(x,\mu,\xi). \tag{20}$$

Since, in Landau gauge, $\tilde{Z}_1(\mu,\Lambda,0) = 1$ for any μ according to Taylor [11], we have

$$\alpha(x) = \alpha(\mu)F(x,\mu,0)G^2(x,\mu,0). \tag{21}$$

Since the functions $F(x)$ and $G(x)$ depend on the momentum, and Eq. (21) is defined for *all* momenta, this evolution yields the *non-perturbative* running coupling in QCD.[1] This expression is renormalization group invariant as the right-hand side of Eq. (21) is independent of the scale μ.

However, we will show that the concept of renormalization scale, as defined in Eqs. (16), (17), can be generalized to what we will call renormalization prescriptions, which correspond to solutions of the nonperturbative field equations. In the derivation of the running coupling, Eqs. (16)–(21), we used the concept *renormalization scale* to describe how the renormalization of the form factors is performed. However, we can interpret Eq. (16) in a more general way, as is sup-

[1]The expression (21) for the nonperturbative running coupling was first proposed by von Smekal *et al.* in Ref. [7].

ported by the symmetries of the nonperturbative equations discussed in Sec. III. The renormalization constants Z_3 and $\tilde{Z}_3$ from Eq. (5) can be scaled by arbitrary real numbers a and b as in Eqs. (13), (14), and still satisfy the renormalization group invariance Eq. (21), even though Eq. (17) will in general no longer be satisfied since it can happen that no renormalization scale μ can be found where $F(\mu)=1=G(\mu)$.

We now clarify this point. Suppose we found renormalization constants $Z_3(\mu,\Lambda,\xi)$ and $\tilde{Z}_3(\mu,\Lambda,\xi)$ such that $F(\mu,\mu,\xi)=1=G(\mu,\mu,\xi)$. To change the renormalization scale from μ to ν we have to scale Z_3 and $\tilde{Z}_3$ so that now $F(\nu,\nu,\xi)=1=G(\nu,\nu,\xi)$. To achieve this, the new renormalization constants have to be

$$Z_3(\nu,\Lambda,\xi)=F(\nu,\mu,\xi)Z_3(\mu,\Lambda,\xi)$$

$$\tilde{Z}_3(\nu,\Lambda,\xi)=G(\nu,\mu,\xi)\tilde{Z}_3(\mu,\Lambda,\xi),$$

which means that the form factors at any momentum x, expressed with two different renormalization scales μ and ν, are related as follows:

$$F(x,\nu,\xi)=F(x,\mu,\xi)/F(\nu,\mu,\xi)$$

$$G(x,\nu,\xi)=G(x,\mu,\xi)/G(\nu,\mu,\xi).$$

Hence, an arbitrary change of renormalization scale from μ to ν corresponds to scalings (13), (14) where

$$a=F(\nu,\mu,\xi), \quad b=G(\nu,\mu,\xi). \tag{22}$$

However, the reasoning followed in Eqs. (16)–(21), using quantities renormalized at a scale μ, can be generalized by applying arbitrary scalings a and b to Z_3 and $\tilde{Z}_3$, provided α is scaled accordingly, so that

$$\alpha(x)=\alpha F(x)G^2(x), \tag{23}$$

remains unchanged for any choice of a and b. The values a and b of Eq. (22) are just special sets and the renormalization scale invariance as shown above in Eq. (21), is only a subgroup of the more general renormalization group invariance summarized in Eq. (23). The renormalized quantities in the right-hand side of Eq. (23) can no longer be regarded as being dependent on a renormalization scale μ, since in general Eq. (17) is no longer satisfied, but correspond to a specific choice of renormalization prescription instead. This more general renormalization group invariance is supported by the results of the nonperturbative integral equations as discussed in Sec. III.

In our nonperturbative treatment the renormalization group invariance corresponds to an invariance of the running coupling with respect to an arbitrary transformation in the three-dimensional space of solutions of the equations. This invariance of $\alpha(x)$ is exactly reproduced in the ghost-loop-only truncation. We will see in Sec. IX that the loss of symmetry of the equations, when we include the gluon loop in the approximation employed, destroys this invariance, and different renormalization prescriptions no longer lead to the same running coupling.

V. INFRARED BEHAVIOR

We will show analytically that Eqs. (9), (10) and Eqs. (11), (12) have a consistent infrared asymptotic solution:

$$F(x)=Ax^{2\kappa} \tag{24}$$

$$G(x)=Bx^{-\kappa}, \tag{25}$$

and that these solutions even solve the *ghost-loop-only* equations (11), (12) exactly for all momenta. Let us try the *Ansatz*

$$F(x)=Ax^{\alpha}, \quad G(x)=Bx^{\beta}. \tag{26}$$

In the infrared asymptotic regime the gluon loop does not contribute to lowest order. Substituting Eq. (26) into the integral equations (11), (12) we calculate

$$A^{-1}x^{-\alpha}=A^{-1}\sigma^{-\alpha}+\lambda\tilde{Z}_1B^2\left[\frac{3}{2}\frac{1}{2+\beta}-\frac{1}{3+\beta}-\frac{1}{4\beta}\right]\times(x^{2\beta}-\sigma^{2\beta}) \tag{27}$$

and

$$B^{-1}x^{-\beta}=B^{-1}\sigma^{-\beta}-\frac{9}{4}\lambda\tilde{Z}_1AB\left[\frac{1}{2+\beta}-\frac{1}{\alpha+\beta}\right]\times(x^{\alpha+\beta}-\sigma^{\alpha+\beta}) \tag{28}$$

on condition that

$$\beta>-2 \tag{29}$$

to avoid infrared singularities. The powers on both sides of Eqs. (27), (28) agree if

$$\alpha=-2\beta,$$

and defining the index κ by

$$\alpha=2\kappa, \quad \beta=-\kappa \tag{30}$$

we find that both the constant and the power terms in Eq. (27) and Eq. (28) match if

$$\lambda\tilde{Z}_1AB^2=\left[\frac{3}{2(2-\kappa)}-\frac{1}{3-\kappa}+\frac{1}{4\kappa}\right]^{-1} \tag{31}$$

and

$$\lambda\tilde{Z}_1AB^2=-\frac{4}{9}\left[\frac{1}{2-\kappa}-\frac{1}{\kappa}\right]^{-1}. \tag{32}$$

Elimination of $\lambda\tilde{Z}_1AB^2$ yields a quadratic equation for κ, which remarkably does not depend on the value of the coupling strength λ:

$$19\kappa^2-77\kappa+48=0, \tag{33}$$

which has two real solutions

$$\kappa = \frac{77 \pm \sqrt{2281}}{38}, \tag{34}$$

or

$$\kappa_1 \approx 0.769479 \quad \text{and} \quad \kappa_2 \approx 3.28315. \tag{35}$$

The second root is spurious: it must be rejected because it gives rise to infrared singularities and thus does not give a solution of the integral equation.

Replacement of κ by κ_1 in Eq. (31) or Eq. (32) yields the condition:

$$\nu = \lambda \tilde{Z}_1 A B^2 \approx 0.912771. \tag{36}$$

From Eq. (23) we know that the running coupling is given by

$$\alpha(x) = 4\pi\lambda F(x) G^2(x) \tag{37}$$

in the Landau gauge. Condition Eq. (36) is important, as it tells us that the running coupling has a non-trivial infrared fixed point

$$\lim_{x \to 0} \alpha(x) \approx 11.4702. \tag{38}$$

This means that the ghost field, which only introduces quantitative corrections to the perturbative ultraviolet behavior of the running coupling, does alter its infrared behavior in a very drastic way.

We will show further on that the running coupling remains almost constant up to a certain momentum scale $\tilde{x}$, after which it decreases as $1/\log x$. The momentum scale at which the constant bends over into a logarithmic tail is closely related to the value of Λ_{QCD}. This is easily understood intuitively, since the perturbative ultraviolet behavior of the running coupling blows up very quickly as the momentum gets down to $\mathcal{O}(\Lambda_{QCD})$.

VI. INFRARED ASYMPTOTIC SOLUTION

Although we have seen in the previous section that the pure power behaviors for $F(x)$ and $G(x)$ solve the reduced equations exactly, these power solutions only give rise to a two-dimensional space of solutions. However, the numerical results told us that the equations were much richer then we initially believed. These numerical results tended to suggest that the power solutions are only one very special two-dimensional family of solutions in the midst of a whole three-dimensional space. Typical non-power solutions showed an infrared behavior completely consistent with the power solution mentioned earlier, which then bends over quite rapidly at some momentum $\tilde{x}$ into a completely different ultraviolet behavior which seemed to be proportional to some power of the logarithm of momentum. A straightforward investigation of the ultraviolet asymptotic behavior of the solutions tells us that such powers of logarithms are indeed consistent ultraviolet solutions, but no obvious mechanism seemed available to match the infrared to the ultraviolet parts of the solutions, making us believe at first that the numerical program was giving us spurious pseudo-solutions, due to some numerical inaccuracies or artifacts. One of the main reasons was that the infrared power behavior only contains one free parameter, and a standard asymptotic expansion does not add any corrections to the leading power. If the infrared asymptotic solution contains only one parameter, it was very unclear how an infinite number of solutions with log-tails could develop out of each power solution. Nevertheless the numerical results indicated that each power solution had an infinite number of corresponding log-tailed solutions, and each solution seemed to be characterized by the momentum at which the log-tail sets in.

The traditional asymptotic expansion one would normally try, is as follows:

$$F(x) = x^{2\kappa} \sum_{i=0}^{N} A_i x^i \tag{39}$$

$$G(x) = x^{-\kappa} \sum_{i=0}^{N} B_i x^i. \tag{40}$$

The reason for this is that each term in the expansion usually generates terms, through integration, that are of the same power or one unit higher. However, the fact that the equations under consideration are *exactly* solved by the power solution alters the reasoning. The leading power term does not generate additional, next-to-leading order terms, and all A_i, B_i for $i > 0$ have to be zero for consistency reasons.

However, the fact that the power solution solves the integral equations does not mean that this is the unique solution, and we next tried an infrared asymptotic solution of the shape:

$$F(x) = A_0 x^{2\kappa} + A_1 x^{\alpha_1}$$

$$G(x) = B_0 x^{-\kappa} + B_1 x^{\beta_1} \tag{41}$$

with $\alpha_1 > 2\kappa$ and $\beta_1 > -\kappa$. Substitution of these solutions into Eqs. (11), (12), tells us that consistency is obtained if $\alpha_1 - \beta_1 = \kappa$, as for the leading power, but it gives an additional constraint, fixing the value of the exponent of the next-to-leading exponent. However, the solution proposed above does generate additional higher order terms, and consistent asymptotic infrared expansions can be built as follows:

$$F(x) = x^{2\kappa} \sum_{i=0}^{N} A_i x^{i\rho}$$

$$G(x) = x^{-\kappa} \sum_{i=0}^{N} B_i x^{i\rho}, \tag{42}$$

where the exponents of successive powers always increase by the same amount $\rho > 0$. To check the consistency of these infrared asymptotic expansions, we substitute them into Eqs. (11), (12). We make a Taylor expansion of the left-hand sides of these equations and expand the series multiplications, before integration, on the right-hand sides. Consis-

tency requires that the coefficients of equal powers of momentum match each other on both sides of the equations.

The conditions on the leading term remain unchanged as described in Sec. V, with $\kappa \approx 0.769479$ and $\nu = \lambda \tilde{Z}_1 A_0 B_0^2 \approx 0.912771$. Equating the second order terms on left- and right-hand sides of both integral equations yields the following set of two *homogeneous* linear algebraic equations for $a_1 \equiv A_1/A_0$ and $b_1 \equiv B_1/B_0$:

$$\frac{a_1}{\nu} + \left(\frac{3}{2(2-\kappa+\rho)} - \frac{1}{3-\kappa+\rho} + \frac{3}{2(2-\kappa)} - \frac{1}{3-\kappa} - \frac{1}{-2\kappa+\rho} \right) b_1 = 0$$

$$\times \left(\frac{1}{\kappa+\rho} - \frac{1}{2-\kappa} \right) a_1 + \left(\frac{1}{\kappa+\rho} - \frac{1}{2-\kappa+\rho} + \frac{4}{9\nu} \right) b_1 = 0.$$

This set of equations will only have non-trivial solutions if its determinant is zero, in which case it will have a one-parameter infinite number of solutions. The characteristic equation is

$$-9.27685\rho^4 - 15.5544\rho^3 + 30.2899\rho^2 + 71.5686\rho = 0. \tag{43}$$

The four solutions are:

$$\rho = 0, \quad \rho = 1.96964, \quad \rho = -1.82316 \pm 0.770012i. \tag{44}$$

The solution $\rho = 0$ corresponds to the pure power solution. The two complex solutions are spurious as they are not consistent with $\mathrm{Re}\,\rho > 0$, while the solution $\rho = 1.96964$ gives rise to consistent infrared asymptotic expansions.

The linear homogeneous set of equations then yields

$$\eta \equiv b_1/a_1 = 0.829602, \tag{45}$$

and the solutions of this set of equations can, for instance, be parametrized by a_1.

Let us define

$$a_n = A_n/A_0, \quad b_n = B_n/B_0, \tag{46}$$

in terms of which we find the following *heterogeneous* set of equations for a_2 and b_2:

$$\frac{a_2}{\nu} + \left[\frac{3}{2(2-\kappa)} - \frac{1}{3-\kappa} + \frac{3}{2(2-\kappa+2\rho)} - \frac{1}{3-\kappa+2\rho} - \frac{1}{-2\kappa+2\rho} \right] b_2$$

$$= \frac{a_1^2}{\nu} - \left(\frac{3}{2(2-\kappa+\rho)} - \frac{1}{3-\kappa+\rho} - \frac{1}{2(-2\kappa+2\rho)} \right) b_1^2$$

$$\times \left[\frac{1}{\kappa+2\rho} - \frac{1}{2-\kappa} \right] a_2 + \left[\frac{1}{\kappa+2\rho} - \frac{1}{2-\kappa+2\rho} + \frac{4}{9\nu} \right] b_2$$

$$= \frac{4b_1^2}{9\nu} - \left(\frac{1}{\kappa+2\rho} - \frac{1}{2-\kappa+\rho} \right) a_1 b_1, \tag{47}$$

with unique solution

$$a_2 = 0.408732 a_1^2, \quad b_2 = 1.31169 a_1^2$$

and for a_3, b_3:

$$\frac{a_3}{\nu} + \left[\frac{3}{2(2-\kappa)} - \frac{1}{3-\kappa} + \frac{3}{2(2-\kappa+3\rho)} - \frac{1}{3-\kappa+3\rho} - \frac{1}{-2\kappa+3\rho} \right] b_3$$

$$= \frac{2a_1a_2 - a_1^3}{\nu} - \left[\frac{3}{2(2-\kappa+2\rho)} - \frac{1}{3-\kappa+2\rho} \frac{3}{2(2-\kappa+\rho)} - \frac{1}{3-\kappa+\rho} - \frac{1}{-2\kappa+3\rho} \right] b_1 b_2 \left[\frac{1}{\kappa+3\rho} - \frac{1}{2-\kappa} \right] a_3$$

$$+ \left[\frac{1}{\kappa+3\rho} - \frac{1}{2-\kappa+3\rho} + \frac{4}{9\nu} \right] b_3$$

$$= \frac{4(2b_1b_2 - b_1^3)}{9\nu} - \left(\frac{1}{\kappa+3\rho} - \frac{1}{2-\kappa+2\rho} \right) a_1 b_2 - \left(\frac{1}{\kappa+3\rho} - \frac{1}{2-\kappa+\rho} \right) a_2 b_1 \tag{48}$$

with unique solution

$$a_3 = -0.761655 a_1^3, \quad b_3 = 0.783905 a_1^3.$$

By induction one can prove that the higher order terms all yield sets of equations of the same nature as Eq. (47) and Eq. (48), where the right-hand side of the set defining the coefficients a_n, b_n are proportional to a_1^n. This means that we have a general solution for the nth order coefficient of the type

$$a_n = f_n a_1^n, \quad b_n = g_n a_1^n \tag{49}$$

for $n > 1$, where the f_n, g_n are constants (independent of λ and of $\tilde{Z}_1$).

The asymptotic expansions Eq. (42) can thus be written in the form

$$F(x)=A_0x^{2\kappa}\left(1+\sum_{i=1}^{N} f_i a_1^i x^{i\rho}\right)$$

$$G(x)=B_0x^{-\kappa}\left(1+\sum_{i=1}^{N} g_i a_1^i x^{i\rho}\right), \tag{50}$$

where A_0, B_0 and $a_1=A_1/A_0$ are chosen to be the free parameters spanning the whole three-dimensional space of solutions of Eqs. (11), (12) in the infrared region, and where (to 6 significant figures)

$$\nu\equiv\lambda\tilde{Z}_1A_0B_0^2=0.912771, \qquad \kappa=0.769479, \qquad \rho=1.96964$$

$$f_1=1, \qquad f_2=0.408732, \qquad f_3=-0.761655,\ldots$$

$$g_1=\eta\equiv b_1/a_1=0.829602, \qquad g_2=1.31169, \qquad g_3=0.783905,\ldots\ . \tag{51}$$

It is precisely the existence of a third independent parameter, namely a_1, which allows the infrared power solution to bend over in a logarithmic tail in a way consistent with the integral equations. To build a solution that is both consistent with the infrared asymptotic expansion set up in this section and the asymptotic ultraviolet logarithmic behavior which will be derived in the next section, the parameter a_1 has to be negative, as has been inferred from the numerical results calculated with the Runge-Kutta method and with the direct integral equation method. If $a_1=0$ we retrieve the pure power solution and if $a_1>0$ there does not seem to be a singularity-free solution for $x\in[0,\Lambda^2]$.

As we have shown in Sec. III, the three-dimensional family of solutions can also be constructed once we have found one solution, just by relying on the three distinct scale invariances (13), (14), (15). How these scale invariances correspond to choices of infrared asymptotic parameters will now be elucidated.

The function scalings (13), (14) of $F(x),G(x)$ correspond to similar scalings of A_0,B_0 in the infrared expansions Eq. (50),

$$\tilde{A}_0=A_0/a, \quad \tilde{B}_0=B_0/b,$$

such that condition Eq. (51) remains satisfied with $\tilde{\lambda}=\lambda ab^2$, and a_1 is left unchanged.

Less trivial is the momentum scaling invariance of the space of solutions:

$$\hat{F}(x)\equiv F(tx), \quad \hat{G}(x)\equiv G(tx). \tag{52}$$

Using these definitions in Eq. (50), we find, after some rearrangement,

$$\hat{F}(x)=(t^{2\kappa}A_0)x^{2\kappa}\left(1+\sum_{i=1}^{N} f_i(t^\rho a_1)^i x^{i\rho}\right)$$

$$\hat{G}(x)=(t^{-\kappa}B_0)x^{-\kappa}\left(1+\sum_{i=1}^{N} g_i(t^\rho a_1)^i x^{i\rho}\right).$$

This shows that the infrared expansions for the momentum scaled functions $\hat{F}(x),\hat{G}(x)$ correspond to asymptotic expansions parametrized by

$$\hat{A}_0=t^{2\kappa}A_0, \quad \hat{B}_0=t^{-\kappa}B_0 \quad \text{and} \quad \hat{a}_1=t^\rho a_1, \tag{53}$$

and that the asymptotic expansions indeed obey Eq. (50) and the conditions Eq. (51). As we expected, there is a one-to-one correspondence between the solutions constructed from the scaling invariances based on the symmetries of the equations, and the parameters A_0, B_0 and a_1 characterizing their infrared expansions.

Let us now construct the asymptotic expansion of the running coupling (with $\tilde{Z}_1=1$) using the expansions (50):

$$\lambda(x)=\lambda F(x)G^2(x)$$
$$=\lambda A_0B_0^2\left(1+\sum_{i=1}^{N} f_i a_1^i x^{i\rho}\right)\left[\left(1+\sum_{i=1}^{N} g_i a_1^i x^{i\rho}\right)\right]^2 \tag{54}$$

or (again truncating at N)

$$\lambda(x)=\nu\left(1+\sum_{i=1}^{N} h_i a_1^i x^{i\rho}\right), \tag{55}$$

where

$$h_1=2.65920, \quad h_2=5.37956, \quad h_3=6.97232,\ldots,$$

which tells us that the running coupling only depends on the dimensionful parameter $a_1\equiv A_1/A_0$, and is independent of λ, A_0 and B_0. Furthermore, we can show from Eqs. (52), (53) that the running coupling corresponding to the parameter $\tilde{a}_1$, is identical to the running coupling with parameter

a_1 after scaling the momentum with a factor $t=(\tilde{a}_1/a_1)^{1/\rho}$. This tells us that the momentum units of a_1 are unambiguously related to the physical scale of the experimentally determined running coupling.

We now introduce a momentum scale Ω^2:

$$\Omega^2=\frac{1}{(h_1|a_1|)^{1/\rho}} \tag{56}$$

(recall that $a_1<0$), such that

$$\lambda(x)=\nu\left(1+\sum_{i=1}^{N}(-1)^i\tilde{h}_i\left(\frac{x}{\Omega^2}\right)^{i\rho}\right), \tag{57}$$

where we defined

$$\tilde{h}_i=\frac{h_i}{h_1^i}: \quad \tilde{h}_1=1, \quad \tilde{h}_2=0.760753, \quad \tilde{h}_3=0.370785,\ldots .$$

We will see from the numerical results that Ω^2 is a good estimate of the scale up to which the infrared asymptotic expansion remains valid.

VII. ULTRAVIOLET BEHAVIOR

We now turn to the investigation of the ultraviolet asymptotic behavior of the solutions. As discussed before, the numerical results show a three-dimensional space of solutions, which has been confirmed by an analytical study of the global symmetries of the integral equations and by the study of the infrared asymptotic expansions of the solutions. Except for the pure power solution, all these solutions bend over in a log-tail above a certain momentum scale x. We will now check the consistency of such ultraviolet logarithmic solutions.

Suppose the solutions for $F(x)$ and $G(x)$, taking on the values F_μ and G_μ at some momentum μ in the perturbative regime, have the following ultraviolet behavior:

$$F(x)\equiv F_\mu\left[\omega\,\log\left(\frac{x}{\mu}\right)+1\right]^{\gamma} \tag{58}$$

$$G(x)\equiv G_\mu\left[\omega\,\log\left(\frac{x}{\mu}\right)+1\right]^{\delta}. \tag{59}$$

We check the consistency of these ultraviolet solutions by substituting these expressions in Eqs. (11), (12), thus determining the values of γ, δ and ω.

The ghost equation (12) yields, to leading log,

$$G_\mu^{-1}\left[\omega\,\log\left(\frac{x}{\mu}\right)+1\right]^{-\delta} = G_\mu^{-1}\left[\omega\,\log\left(\frac{\sigma}{\mu}\right)+1\right]^{-\delta}-\frac{9}{4}\lambda\tilde{Z}_1F_\mu G_\mu \times\int_x^\sigma\frac{dy}{y}\left[\omega\,\log\left(\frac{y}{\mu}\right)+1\right]^{\gamma+\delta}. \tag{60}$$

After evaluating the integral we get

$$G_\mu^{-1}\left[\omega\,\log\left(\frac{x}{\mu}\right)+1\right]^{-\delta} = G_\mu^{-1}\left[\omega\,\log\left(\frac{\sigma}{\mu}\right)+1\right]^{-\delta}-\frac{9\lambda\tilde{Z}_1F_\mu G_\mu}{4\omega(\gamma+\delta+1)} \times\left\{\left[\omega\,\log\left(\frac{\sigma}{\mu}\right)+1\right]^{\gamma+\delta+1}-\left[\omega\,\log\left(\frac{x}{\mu}\right)+1\right]^{\gamma+\delta+1}\right\}. \tag{61}$$

Matching the index of the leading powers of logarithms in Eq. (61) one finds the consistency condition:

$$\gamma+2\delta=-1 \tag{62}$$

and, equating the leading log coefficients in Eq. (61), using Eq. (62), we get

$$\lambda\tilde{Z}_1F_\mu G_\mu^2=\frac{2\omega}{9}(\gamma+1). \tag{63}$$

Substituting the solutions Eqs. (58), (59) in the gluon equation Eq. (11) and keeping only the leading log terms, we find

$$F_\mu^{-1}\left[\omega\,\log\left(\frac{x}{\mu}\right)+1\right]^{-\gamma} = F_\mu^{-1}\left[\omega\,\log\left(\frac{\sigma}{\mu}\right)+1\right]^{-\gamma} +\lambda\tilde{Z}_1G_\mu^2\int_x^\sigma\frac{dy}{2y}\left[\omega\,\log\left(\frac{y}{\mu}\right)+1\right]^{2\delta}. \tag{64}$$

After performing the integrals, we find

$$F_\mu^{-1}\left[\omega\,\log\left(\frac{x}{\mu}\right)+1\right]^{-\gamma} = F_\mu^{-1}\left[\omega\,\log\left(\frac{\sigma}{\mu}\right)+1\right]^{-\gamma}+\frac{\lambda\tilde{Z}_1G_\mu^2}{2\omega(2\delta+1)} \times\left\{\left[\omega\,\log\left(\frac{\sigma}{\mu}\right)+1\right]^{2\delta+1}-\left[\omega\,\log\left(\frac{x}{\mu}\right)+1\right]^{2\delta+1}\right\}. \tag{65}$$

Consistency of the exponents on both sides of the equation is automatically guaranteed by Eq. (62). Then, equating the coefficients of the leading log contributions of Eq. (65), and substituting Eq. (62), we obtain

$$\lambda\tilde{Z}_1F_\mu G_\mu^2=2\omega\gamma. \tag{66}$$

From Eqs. (62), (63), (66) we then find

$$\gamma=\frac{1}{8}, \quad \delta=-\frac{9}{16} \tag{67}$$

and the equivalent conditions Eqs. (63), (66) yield

$$\omega = 4\lambda \tilde{Z}_1 F_\mu G_\mu^2 . \tag{68}$$

Thus, the ultraviolet solutions for $F(x), G(x)$ can be written as

$$F(x) = F_\mu \left[4\lambda \tilde{Z}_1 F_\mu G_\mu^2 \log\left(\frac{x}{\mu}\right) + 1 \right]^{1/8} \tag{69}$$

$$G(x) = G_\mu \left[4\lambda \tilde{Z}_1 F_\mu G_\mu^2 \log\left(\frac{x}{\mu}\right) + 1 \right]^{-9/16} \tag{70}$$

and the renormalization group invariant running coupling is given by

$$\lambda(x) = \lambda F(x) G^2(x) = \frac{1}{4\tilde{Z}_1 \log\left(\frac{x}{\mu}\right) + \frac{1}{\lambda F_\mu G_\mu^2}} . \tag{71}$$

We can rewrite this in the form

$$\lambda(x) = \frac{1}{\beta_0 \log\left(\frac{x}{\Lambda_{QCD}^2}\right)}, \tag{72}$$

where $\beta_0 = 4$, and the QCD scale is given by

$$\Lambda_{QCD}^2 = \mu \exp\left(-\frac{1}{4\lambda F_\mu G_\mu^2} \right), \tag{73}$$

if $\tilde{Z}_1 = 1$. We see that fixing $\lambda F_\mu G_\mu^2$ at a scale μ, in the perturbative regime, indeed amounts to a definition the value of Λ_{QCD}.

The leading log coefficient is $\beta_0 = 4$, but this is not in agreement with perturbation theory, where $\beta_0 = 11$. However, the reason for this is obvious, as we only considered the ghost loop and discarded the gluon loop in the gluon equation.

VIII. RESULTS

Knowing the infrared and ultraviolet asymptotic behaviors of the coupled equations (11), (12), we now go on to solve the equations numerically in order to see if we can find consistent solutions over the whole momentum range, connecting both asymptotic regions, hopefully giving us more insight into the transition from the regime of asymptotic freedom to the state of confinement.

We use a numerical method developed by one of us for the study of dynamical fermion mass generation in QED_4 [12]. This method, which directly solves the coupled integral equations by an iterative numerical scheme, is explained in more detail in Appendix B.

Using this method, we performed a meticulous study of the equations Eqs. (11), (12). We note that, for a fixed value of λ, the equations have two free parameters, for instance $F(\sigma)$ and $G(\sigma)$ [restricted by Eq. (36), $\lambda F(\sigma) G^2(\sigma) \leqslant 0.912771$] Furthermore, as shown in Sec. III, a scaling of λ can always be absorbed in a redefinition of the unknown functions $F(x)$ and $G(x)$, such that knowing the solution space for one value of λ, we can build the solutions for any arbitrary value of λ in a straightforward way. Moreover, such scalings of λ leave the running coupling $\lambda F(x) G^2(x)$ unchanged.

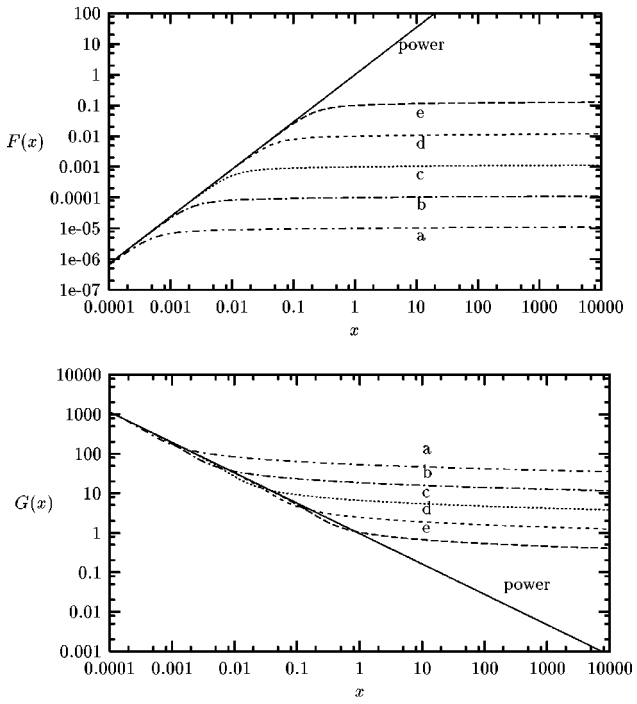

FIG. 1. Gluon and ghost form factors $F(x)$ and $G(x)$ versus momentum x (on log-log plot), for $\lambda = 1$, $A = 1$ and $F_1 = 10^{-5}$(a), 10^{-4}(b), 10^{-3}(c), 0.01(d) and 0.1(e).

In practice, we choose an alternative pair of parameters, $F(\sigma)$ and A, where A is the leading infrared gluon coefficient defined in Eq. (24). The choice of these two parameters is suggested by the numerical solution method described in Appendix B. Indeed, using Eq. (36), the value of A also determines the leading infrared ghost coefficient B, and allows us to compute a quite accurate analytical approximation to the infrared part of the integral over $[0, \epsilon^2]$, if the infrared cutoff ϵ^2 is sufficiently small. The choice of $F(\sigma)$ as second parameter can be viewed as a measure of the deviation from the pure power behavior at momentum σ. We have taken the subtraction scale to be $\sigma = 1$ and varied both parameters A and $F(1) = F_1$ to scan the two parameter space of solutions for a fixed value of $\lambda = 1$ and $\tilde{Z}_1 = 1$. The equations are solved using the iterative solution method outlined in Appendix B, starting from initial guesses constructed in Appendix C. As expected, the results exhibit the scaling invariances discussed in the previous sections.

If we plot the solutions for $F(x)$ and $G(x)$ for various sets (A, F_1), as in Fig. 1, we can check that every solution can be transformed into another one by a unique transformation (t,r) corresponding to a momentum scaling tx and a function scaling $rF(x)$, $G(x)/\sqrt{r}$. The numerical results clearly show the expected power behavior in the infrared region and the logarithmic behavior in the ultraviolet region. The value of the

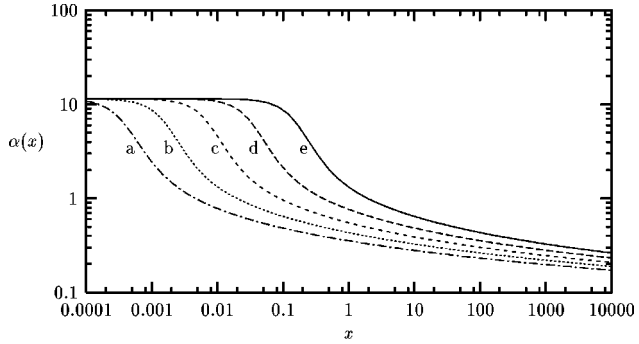

FIG. 2. Running coupling $\alpha(x)=\alpha F(x)G^2(x)$ versus momentum x (on log-log plot), for $A=1$ and $F_1=10^{-5}$(a), 10^{-4}(b), 10^{-3}(c), 0.01(d) and 0.1(e).

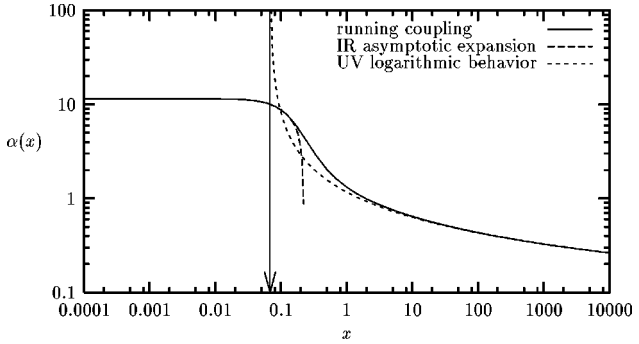

FIG. 3. Running coupling $\alpha F(x)G^2(x)$ versus momentum x (on log-log plot), for parameter values $A=1$ and $F_1=0.1$ together with its infrared asymptotic expansion and its ultraviolet asymptotic behavior.

exponents and of the coefficients in front of the power in the infrared region is completely consistent with the analytical treatment of Sec. V, which was also used to compute the infrared part $[0,\epsilon^2]$ of the integrals analytically. As can be seen from the plots, the gluon form factor, which starts off as a power with a given coefficient A, will bend over at some cross-over point $\tilde{x}$, such that the further logarithmic behavior of the function consistently leads to a value F_1 at the subtraction scale $\sigma=1$. The logarithmic behavior of $F(x)$ and $G(x)$ also satisfies the ultraviolet leading log behavior analyzed in Sec. VII. It is remarkable that both asymptotic regimes, infrared and ultraviolet, seem to connect onto each other at some momentum $\tilde{x}$, with scarcely any intermediate regime.

If we look at the running coupling we see that all the solutions are just translations of each other when plotted on a logarithmic momentum scale, as is illustrated in Fig. 2. This corresponds to the invariance of the space of solutions with respect to scaling of momentum. It also shows the physical equivalence of all solutions as such a transformation can always be absorbed into a redefinition of momentum units.

We also checked the results with a Runge-Kutta method applied to the set of differential equations derived from the integral equations (see Appendix D). Comparison of the results obtained with both methods shows that a very high accuracy can be achieved over quite a broad momentum range (see Appendix E).

It is also interesting to compare the numerical results with the analytic asymptotic calculations in order to investigate in which momentum regions the asymptotic solutions are valid. As example we consider the case $A=1$ and $F_1=0.1$. To compute the infrared asymptotic expansion we need to know the value of the infrared parameter a_1 in Eq. (50). We used the Runge-Kutta method, described in Appendix D, in order to determine the value of a_1 yielding a value of $F(1)=0.1$ for the gluon form factor, with $A=1$. For this specific case, the value is $a_1\approx-10.27685$ or $\Omega^2\approx0.186475$ [from Eq. (56)]. The infrared asymptotic expansion, derived in Sec. VI, is calculated from Eq. (57) and truncated after four terms:

$$\alpha(x)\overset{\text{ir}}{\sim}4\pi\nu\left[1-\left(\frac{x}{\Omega^2}\right)^{\rho}+0.760753\left(\frac{x}{\Omega^2}\right)^{2\rho}-0.370785\left(\frac{x}{\Omega^2}\right)^{3\rho}\right].$$

The ultraviolet asymptotic behavior, derived in Sec. VII, is described by Eq. (72):

$$\alpha(x)\overset{\text{uv}}{\sim}\frac{4\pi}{4\log\left(\frac{x}{\Lambda^2_{QCD}}\right)},$$

where we use Eq. (73),

$$\Lambda^2_{QCD}=\mu\,\exp\left(-\frac{1}{4\lambda(\mu)}\right),$$

to compute the value of Λ_{QCD} for the case under consideration. We choose μ in the perturbative regime, for example $\mu=1032.15$, where the numerical results yield $\lambda(\mu)\equiv\lambda F(\mu)G^2(\mu)\approx0.0259676$, and find

$$\Lambda^2_{QCD}=0.06802,$$

still in arbitrary units, which should be fixed after comparison of the numerical results with experimental data. Because of the incorrect leading log perturbative β-coefficient of the ghost-loop-only truncation (see Sec. VII) we will not actually fix the units as this would give a far too low value of Λ_{QCD}.

In Fig. 3 we plot the running coupling versus momentum, together with its infrared asymptotic expansion and the ultraviolet asymptotic behavior. The agreement between the analytical and numerical results is extremely good, and it can be seen that both asymptotic behaviors flow into each other, almost without any intermediate regime. The vertical line in Fig. 3 situates the scale of Λ^2_{QCD}. We see that Λ^2_{QCD} lies in the momentum regime where the infrared asymptotic expansion has already taken over from the logarithmic behavior, and where the running coupling has become almost constant. Furthermore, the infrared scale $\Omega^2\approx0.186$ seems to be a good measure to delimit the infrared region where the asymptotic expansion is valid.

We can even give a numerical relation between Ω^2 and Λ^2_{QCD} (where the latter is computed from leading log only), namely

$$\frac{\Lambda_{QCD}^2}{\Omega^2} \approx 2.74,$$

and the ratio is the same for all solutions of the equations (11), (12). The simple relation between Ω and Λ_{QCD} is a consequence of the symmetries of the *ghost-loop-only* truncation. If we include the gluon loop, with a bare triple gluon vertex and $Z_1 = 1$, the asymptotic expansion of the running coupling will no longer depend on a_1 alone, but on the other parameters of the infrared expansions as well. Hence an ultraviolet renormalization, leading to a specific value of Λ_{QCD}^2, will correspond to a family of running couplings, all having slightly different behaviors in the intermediate regime, and there will be an ambiguity in the determination of the non-perturbative running coupling. This is a consequence of the violation of renormalization group invariance in that truncation, which implies that different solutions of the equations will correspond to couplings running in different ways.

IX. INCLUDING THE GLUON LOOP

We will now briefly discuss Eqs. (9), (10), i.e. the equations where both gluon loop and ghost loop are included in the gluon equation. Although it is this specific truncation which attracted our attention when we started the investigation of the coupled gluon-ghost equations, the requirements of renormalization group invariance were better met by omitting the gluon loop. As discussed in the previous sections, the ghost-loop-only truncation yielded an unambiguous running coupling, determined by one physically relevant parameter, Λ_{QCD}. In the following subsections, we will briefly show what changes occur when we do include the gluon loop and why an ambiguity occurs.

A. Symmetries of the equations

We can repeat the analysis of Sec. III in the truncation we are considering now. It is easy to see that the solution space will still be invariant under scaling of momentum (15), i.e. when scaling the momentum of any solution of the equations, we retrieve another solution of the same equations. However, the two-parameter scaling invariance (13), (14), with respect to the functions themselves, is now reduced to a one-parameter scaling invariance because of the additional constraint $a = b$ on the scaling factors, which comes from adding the gluon loop. While the *ghost-loop-only* case was solely a function of products $F(x)G(y)G(z)$, for various combinations of x,y,z, the current truncation depends on $F(x)F(y)F(z)$ as well as on $F(x)G(y)G(z)$. The fact that the three-dimensional space of solutions has lost part of its symmetry is important, as it means that $\lambda F(x)G^2(x)$ is not unique, even after an appropriate scaling of momentum. Globally we can say that $\lambda F(x)G^2(x)$ is no longer invariant, because of the admixture of $\lambda F^3(x)$ terms. However, even in the absence of the three-fold symmetry, after inclusion of the gluon loop, the coupled equations still have a three-dimensional manifold of solutions. The only difference being that only two of the three dimensions of the solution space can be reached by simple symmetry operations, while the third dimension now corresponds to deformations of the solutions.

It is important to note that the loss of symmetry is entirely due to the weakness of the truncation. The exact inclusion of gluon loop, i.e. using the exact full triple gluon vertex and the exact renormalization constant Z_1, will lead to a recovery of the three-fold symmetry exhibited by the ghost-loop-only truncation.

B. Infrared behavior

Because the ghost equation remains unchanged, it is easy to see that the leading infrared behavior in this case will be the same as in the *ghost-loop-only* case. The additional gluon loop in the gluon equation only yields higher order corrections. The asymptotic expansion set up in Sec. VI is still generated in this case, but at some higher order it will have to be supplemented by other higher order series, which will be related to the leading asymptotic series. We also note that the power solution will not be an exact solution of the equations any more, although it remains the correct leading infrared asymptotic behavior.

C. Ultraviolet behavior

We will show that the leading log ultraviolet behavior of the running coupling still has the $1/\log x$ behavior, as expected from perturbation theory, but that the β-coefficient is different from the perturbative one. This discrepancy is a bit surprising, since one expects the perturbative result to be contained in the ghost and gluon equations considered. The reason why this happens is that, for some reason, the pure perturbative result does not consistently solve the non-perturbative equations.

As in Sec. VII, we try the following ultraviolet solutions for $F(x)$ and $G(x)$, taking on the values F_μ and G_μ at some momentum μ in the perturbative regime:

$$F(x) \equiv F_\mu \left[\omega \log\left(\frac{x}{\mu}\right) + 1 \right]^\gamma \tag{74}$$

$$G(x) \equiv G_\mu \left[\omega \log\left(\frac{x}{\mu}\right) + 1 \right]^\delta . \tag{75}$$

We check the consistency of these ultraviolet solutions by substituting the expressions in Eqs. (9), (10). For the ghost equation, Eq. (10), the treatment is identical to that of Sec. VII and we again have

$$\gamma + 2\delta = -1, \tag{76}$$

and

$$\lambda \tilde{Z}_1 F_\mu G_\mu^2 = \frac{2\omega}{9}(\gamma + 1). \tag{77}$$

Substituting the solutions Eqs. (74), (75) in the gluon equation Eq. (9) and keeping only the leading log terms, we now find

$$F_\mu^{-1}\left[\omega\,\log\left(\frac{x}{\mu}\right)+1\right]^{-\gamma} = F_\mu^{-1}\left[\omega\,\log\left(\frac{\sigma}{\mu}\right)+1\right]^{-\gamma} - 7\lambda Z_1 F_\mu^2 \times\int_x^\sigma \frac{dy}{y}\left[\omega\,\log\left(\frac{y}{\mu}\right)+1\right]^{2\gamma} + \lambda\tilde{Z}_1 G_\mu^2\int_x^\sigma\frac{dy}{2y}\left[\omega\,\log\left(\frac{y}{\mu}\right)+1\right]^{2\delta}. \quad (78)$$

After evaluation of the integrals and substitution of Eq. (76),

$$F_\mu^{-1}\left[\omega\,\log\left(\frac{x}{\mu}\right)+1\right]^{-\gamma} = F_\mu^{-1}\left[\omega\,\log\left(\frac{\sigma}{\mu}\right)+1\right]^{-\gamma} - \frac{7\lambda Z_1 F_\mu^2}{\omega(2\gamma+1)} \times\left\{\left[\omega\,\log\left(\frac{\sigma}{\mu}\right)+1\right]^{2\gamma+1} - \left[\omega\,\log\left(\frac{x}{\mu}\right)+1\right]^{2\gamma+1}\right\} - \frac{\lambda\tilde{Z}_1 G_\mu^2}{2\omega\gamma}\left\{\left[\omega\,\log\left(\frac{\sigma}{\mu}\right)+1\right]^{-\gamma} - \left[\omega\,\log\left(\frac{x}{\mu}\right)+1\right]^{-\gamma}\right\}. \quad (79)$$

Consistency of this equation requires $\gamma \leqslant -1/3$, in order to equate the leading log terms on both sides of the equation. We first consider the case $\gamma < -1/3$, for which the gluon loop does not contribute to leading log. Then, the consistency of Eq. (79) requires that

$$\lambda\tilde{Z}_1 F_\mu G_\mu^2 = 2\omega\gamma. \quad (80)$$

From Eqs. (77), (80) we then find

$$\gamma = \frac{1}{8} \not< -\frac{1}{3}, \quad (81)$$

which is inconsistent with the initial assumption $\gamma < -1/3$. The only possibility left is

$$\gamma = -1/3, \quad (82)$$

for which both the gluon and the ghost loop contribute to leading order. From Eq. (76) we then also find

$$\delta = -1/3, \quad (83)$$

and the condition Eq. (77) derived from the ghost equation yields

$$\omega = \frac{27}{4}\lambda\tilde{Z}_1 F_\mu G_\mu^2. \quad (84)$$

Equation (79) then becomes

$$F_\mu^{-1}\left[\omega\,\log\left(\frac{x}{\mu}\right)+1\right]^{1/3} = F_\mu^{-1}\left[\omega\,\log\left(\frac{\sigma}{\mu}\right)+1\right]^{1/3} + \frac{\lambda}{\omega}\left[-21 Z_1 F_\mu^2 + \frac{3}{2}\tilde{Z}_1 G_\mu^2\right] \times\left\{\left[\omega\,\log\left(\frac{\sigma}{\mu}\right)+1\right]^{1/3} - \left[\omega\,\log\left(\frac{x}{\mu}\right)+1\right]^{1/3}\right\}, \quad (85)$$

which leads to the condition:

$$\omega = \lambda\left[21 Z_1 F_\mu^3 - \frac{3}{2}\tilde{Z}_1 F_\mu G_\mu^2\right]. \quad (86)$$

Equations (84), (86) give us

$$G_\mu^2 = \frac{28 Z_1}{11\tilde{Z}_1} F_\mu^2, \quad (87)$$

which is a relation between the leading log renormalized values of F_μ and G_μ, when the renormalization scale μ is in the perturbative regime, in which the leading log dominates. This might seem to be in contradiction to perturbation theory, where the values of the renormalized quantities can take an arbitrary value and are usually fixed to 1. However, Eq. (87) still contains the renormalization constants Z_1 and $\tilde{Z}_1$. Taylor has shown that $\tilde{Z}_1 \equiv 1$ in the Landau gauge [11], but one could still hope to be able to achieve the arbitrary renormalization of F and G by a suitable choice of Z_1.

If we write the far UV behavior of $F(x)$ and $G(x)$ as

$$F(x) \sim C\,\log^{-1/3} x \quad \text{and} \quad G(x) \sim D\,\log^{-1/3} x, \quad (88)$$

then, from Eqs. (74), (75), (84), (87), the log-coefficients C and D of $F(x)$ and $G(x)$ are given by

$$C = F_\mu \omega^{-1/3} = \frac{1}{3}\left(\frac{7\lambda Z_1}{11}\right)^{-1/3} \quad (89)$$

and

$$D = G_\mu \omega^{-1/3} = \frac{2}{3}\left(\frac{11\lambda^2\tilde{Z}_1^3}{7 Z_1}\right)^{-1/6}. \quad (90)$$

It is interesting to note that these leading log coefficients are independent of the values F_μ and G_μ if we take $Z_1 = \tilde{Z}_1 = 1$, and therefore this truncation contradicts the requirements of renormalization group invariance.

Let us now look at the ultraviolet behavior of the running coupling. Using the solutions Eqs. (74), (75) and substituting Eq. (84), we find

$$\alpha F(x) G^2(x) = \frac{\alpha F_\mu G_\mu^2}{\frac{27}{4}\lambda\tilde{Z}_1 F_\mu G_\mu^2 \log\left(\frac{x}{\mu}\right)+1}. \quad (91)$$

Now, divide numerator and denominator by $\lambda F_\mu G_\mu^2$:

$$\alpha F(x)G^2(x)=\frac{4\pi}{\frac{27}{4}\tilde{Z}_1\log\left(\frac{x}{\mu}\right)+\frac{1}{\lambda F_\mu G_\mu^2}}, \tag{92}$$

which can be written in the familiar form

$$\alpha F(x)G^2(x)=\frac{4\pi}{\beta_0\log\left(\frac{x}{\Lambda_{QCD}^2}\right)}. \tag{93}$$

The leading log coefficient, $\beta_0=27/4$ if $\tilde{Z}_1=1$, is not in agreement with perturbation theory, for which $\beta_0=11$. This seems somewhat puzzling, because all the one-loop perturbative ingredients are contained in our truncation of the nonperturbative equations, and indeed the leading log perturbative results can be retrieved from a perturbative expansion of these equations. However, the leading log ultraviolet behavior of the *nonperturbative* solutions does not coincide with the leading log perturbative results. This is in contrast to the *ghost-loop-only* truncation, where the leading log ultraviolet behavior of the *nonperturbative* solutions yields a β-coefficient that is identical to that of the perturbative ghost-loop-only calculation.

To show how this disagreement arises, we will briefly discuss the difference in the determination of the ultraviolet behavior of the nonperturbative solutions in both approximations, with and without gluon loop. In the ghost-loop-only case we saw in Sec. VII that the anomalous dimensions of $F(x)$ and $G(x)$ are determined by equating the *coefficients* of the leading logs in the integral equations, as the consistency of the log-exponents on left- and right-hand sides of both equations is automatically guaranteed. When we include the gluon loop the situation is different and the anomalous dimensions are determined by the consistency requirements of the log-exponents. The equality of the coefficients of the leading log terms yields an additional constraint given by Eq. (87). It is this difference in the way of determining the anomalous dimensions that seems to be responsible for the contradiction between perturbative and nonperturbative results when we include the gluon-loop. Although our truncation approximates the full vertices by bare ones and sets $Z_1=1$, the question whether the ultraviolet behavior of the full nonperturbative solution coincides with the results of perturbation theory remains an important issue which we will investigate in the future.

D. Results

We solved Eqs. (9), (10) with $\lambda=1$ and $Z_1=\tilde{Z}_1=1$, for widely varying values of the parameters A and F_1 in order to scan the two-parameter space of solutions for a given λ. However, the loss of symmetry seems to cut out part of the solution space. Although we have made a rather thorough investigation of this, we will not swamp the paper with a detailed discussion since we think that this loss of symmetry is unphysical, thus making this truncation less interesting than the *ghost-loop-only* truncation. To put it briefly, the fact that the ultraviolet behaviors of $F(x)$ and $G(x)$ are independent of $F(\mu)$ and $G(\mu)$ destroys the invariance of the running coupling with respect to the choice of the individual renormalizations of F and G. Hence, choosing $F(\mu)$ too large will prohibit the construction of a consistent solution having the correct ultraviolet asymptotic behavior. For $F(\mu)$ small this is not an obstacle, as we can show that there is an intermediate regime, where the log of momentum takes a different power, which allows us to connect to the correct ultraviolet behavior.

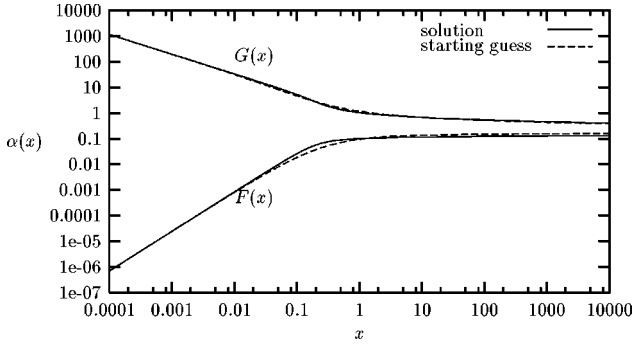

FIG. 4. Gluon form factor $F(x)$ versus momentum x (on log-log plot), for $A=1$ and $F_1=0.001$(a), 0.01(b), 0.1(c), 0.3(d) and 0.5(e).

To see this we plot $F(x)$ for $A=1$ and $F_1=0.001$, 0.01, 0.1, 0.3 and 0.5 in Fig. 4. It is clear that the gluon form factor, which starts off as a power $Ax^{2\kappa}$, bends over at the cross-over point $\tilde{x}$, such that the further logarithmic behavior of the function leads to a value F_1 at the subtraction scale $x=1$. From this plot it is however clear that the curves (d, e) have a quite different behavior from the others. Their ultraviolet behavior is consistent with the $\log^{-1/3}$ analytic prediction from Sec. IX C, while the other curves seem to show a logarithmic increase instead. This is of course plausible, as it is possible that the ultraviolet asymptotic behavior only sets in at much higher momenta, and that in between the infrared and ultraviolet asymptotic behaviors there is a intermediate regime.

From a careful investigation of the equations, we can even find a consistent analytical description of the intermediate regime, connecting the region of confinement to that of asymptotic freedom, which fits the numerical results extremely well. Consider a case where $|F(\sigma)|\ll|G(\sigma)|$. Then, in the intermediate region, $F(x)G^2(x)\gg F^3(x)$, and the gluon loop will be negligible compared to the ghost loop, in the gluon equation, Eq. (9). Keeping in mind the treatment of Sec. VII, we know that this has a consistent ultraviolet solution $F(x)\sim\log^{1/8}x$ and $G(x)\sim\log^{-9/16}x$, which remains valid all the way down to the region where the power behavior bends over to a logarithmic behavior. Comparison with the numerical results shows that indeed the intermediate regime is very well reproduced by these powers of log. The ultimate ultraviolet behavior of Sec. IX C will only set in at extremely high momentum, after the intermediate regime has allowed the form factors to evolve sufficiently in order to connect to the stringently constrained ultraviolet asymptotic behavior. The connection of the asymptotic infrared regime, the intermediate log behavior and the asymptotic ultraviolet behavior reproduce the numerical result to a good accuracy.

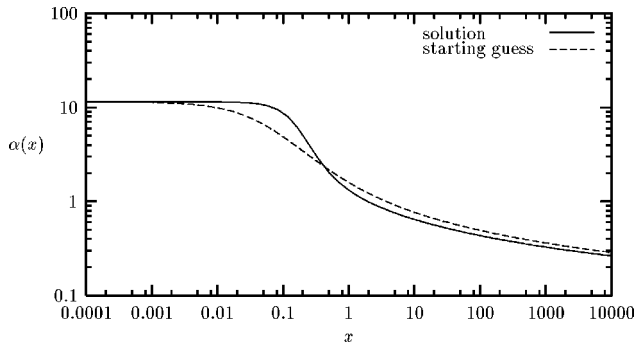

FIG. 5. Running coupling $\alpha(x)$ versus momentum x (on log-log plot), for $A=1$ and $F_1=0.001$(a), 0.01(b), 0.1(c), 0.3(d) and 0.5(e).

To evaluate the relevance of this truncation, it is most interesting to plot the running coupling in Fig. 5. We see that, in contrast to the *ghost-loop-only* truncation of Fig. 2, the various curves for the running coupling are no longer mere translations of each other on log-log scale; and thus, if we choose the units on each curve such that $\alpha(\mu)\equiv\alpha_\mu^{\exp}$, we will find couplings which run in different ways in the intermediate regime. This means that the determination of the running of the strong coupling cannot be determined unambiguously in this case.

X. CONCLUSIONS

Following the study of von Smekal *et al.* [7], where these authors studied the coupled system of Dyson-Schwinger equations for the gluon and ghost propagators, using a Ball-Chiu vertex *Ansatz* for the triple gluon vertex and a Slavnov-Taylor improved form for the gluon-gluon-ghost vertex, we performed a detailed analytical and numerical analysis of the coupled gluon-ghost equations using the *bare* triple gluon and gluon-gluon-ghost vertices. The reason that we went back to the leading-order perturbative vertices was to avoid the ''log x'' problem inherent in the *Ansatz* of Ref. [7]. We have obtained a clear understanding of the mechanism that is the source of the new qualitative behavior of the nonperturbative gluon and ghost propagators and of the running coupling. First, the qualitative changes to the infrared behaviors of the propagators are solely due to the coupling of both propagator equations, and the details of the vertices seem to introduce merely quantitative changes. Secondly, the use of the bare vertices ensures that no infrared singularities occur; hence no additional approximations, except for the vertex *Ansätze* and the y-max approximation, are in principle needed in order to solve these equations.

However, we did apply one more truncation to the coupled gluon-ghost equations. From an analysis of the symmetries of the equations and their solutions, we noted that removing the gluon loop, and keeping only the ghost loop in the gluon equation, leads to a set of equations which is consistent with the renormalization group invariance of the running coupling, while this is not the case in the presence of the gluon loop in the approximations employed.

We performed a detailed analytical and numerical study of the equations with and without the gluon loop. In the case where we removed the gluon loop, we computed the analytical asymptotic infrared expansion, and showed that it depends on three independent parameters defining the infrared behavior of a three-dimensional family of solutions. We also derived the analytic ultraviolet asymptotic behavior of the solutions, which are proportional to powers of logarithms. We then computed the solutions for $F(x)$, $G(x)$ and $\alpha(x)$ over the whole momentum range with two different numerical techniques, the direct solution of the integral equations using a Newton iteration method to find Chebyshev approximations to the unknown functions on the one hand, and on the other hand, the Runge-Kutta method on the set of differential equations derived from the integral equations. The numerical results agree very well with both asymptotic behaviors in the infrared and ultraviolet regions. Furthermore the results of the direct integral equation method and of the Runge-Kutta method agree to a very high accuracy. We found that the equations possess a three-dimensional family of solutions and that they all correspond to one and the same physical running coupling $\alpha(x)=\lambda F(x)G^2(x)$.

We repeated the study with inclusion of the gluon loop, using a bare triple gluon vertex and taking $Z_1=1$, and showed that since renormalization group invariance is now violated, the nonperturbative running coupling cannot be determined unambiguously in this truncation.

To improve on the current study, we should try to incorporate the gluon loop in the gluon equation in a way that respects the physical invariances of the problem. For this, we believe that the bare triple gluon vertex will have to be replaced by an improved vertex, like the Ball-Chiu vertex, and the renormalization constant Z_1 will have to be chosen appropriately. Furthermore it would be interesting to investigate the importance of the y-max approximation.

ACKNOWLEDGMENTS

We thank A. Hams for fruitful discussions. J.C.R.B. was supported by F.O.M. (*Stichting voor Fundamenteel Onderzoek der Materie*).

APPENDIX A: LOG PROBLEM

Let us spell out in more detail the ''log x'' problem inherent in the *Ansatz* of Ref. [7]. With the aforementioned *Ansatz* for the ghost-gluon vertex, one obtains for the ghost form factor

$$G^{-1}(x)=\tilde{Z}_3-\frac{3g^2}{8\pi^3}\tilde{Z}_1\int_0^{\Lambda^2}dyy\int_0^{\pi}d\theta\,\frac{\sin^4\theta}{z^2}F(z)\times\left[G(z)-G(y)+\frac{G(z)G(y)}{G(x)}\right],\tag{A1}$$

where $x=p^2$, $y=q^2$, $z=(p-q)^2$, instead of Eq. (4). The difficulty is that, if one substitutes Eq. (1) into the right hand side of Eq. (A1), one does not produce a behavior $c_1+c_2x^\kappa$, but rather $c_1+x^\kappa[c_2+c_3\log x]$, where the c's are constants. The problematical term is the last one in the square parentheses. In fact, after substitution of the infrared behavior (1),

$$\int_0^{\Lambda^2} dyy \int_0^{\pi} d\theta \, \frac{\sin^4\theta}{z^2} \frac{F(z)G(z)G(y)}{G(x)}$$

$$\sim x^{\kappa} \int_0^{\Lambda^2} dy y^{1-\kappa} \int_0^{\pi} d\theta \, \sin^4\theta z^{\kappa-2}.$$

The θ integral can be evaluated explicitly in terms of the hypergeometric function [9]. We obtain

$$\frac{3\pi}{8} x^{\kappa} \left[\int_0^1 dt t^{1-\kappa} {}_2F_1(2-\kappa,-\kappa;3;t) + \int_{x/\Lambda^2}^1 \frac{dt}{t} \, {}_2F_1(2-\kappa,-\kappa;3;t) \right]$$

and the second of these integrals behaves, for small x and/or large Λ, like $\log \Lambda^2/x$, plus a constant. This is what we mean by the $\log x$ problem. The divergence cannot be absorbed into the renormalization constant $\tilde{Z}_3$, and we conclude that the form (1) is *not* a solution of the equations of Ref. [7], before the angular averaging is made.

The $\log x$ problem persists if one adopts the simple y-max angular averaging as the problematical term becomes

$$\int_x^{\Lambda^2} \frac{dy}{y} \frac{F(y)G^2(y)}{G(x)}.$$

Von Smekal *et al.* circumvent this problem by introducing a modified angular averaging, replacing the form factor $G(x)$ at external momentum x by its value $G(y)$ at radial integration momentum y in the ultraviolet part of the integrals. The term in question then becomes

$$\int_x^{\Lambda^2} \frac{dy}{y} F(y)G(y).$$

Now the $\log x$ problem disappears, but since their equations do not have a solution of the form (1) *before* averaging, it would seem difficult to justify the averaging, since it completely changes the properties of the equation.

APPENDIX B: NUMERICAL METHOD

We give an outline of the main features of the numerical method used to solve the coupled integral equations directly, i.e. without transforming it into a set of differential equations. Unlike most other methods used thus far, we replaced the widely used discretization of the unknown functions by smooth polynomial approximations, introducing Chebyshev expansions for the gluon and ghost form factors $F(x)$ and $G(x)$ and using the logarithm of momentum squared as variable. To improve the accuracy of the Chebyshev approximations we first extract the infrared power behaviors of the form factors, although this only has a minor influence. The form factors are approximated by

$$F(x) \equiv A x^{2\kappa} \left[\frac{a_0}{2} + \sum_{j=1}^{N-1} a_j T_j(s(x)) \right] \tag{B1}$$

$$G(x) \equiv B x^{-\kappa} \left[\frac{b_0}{2} + \sum_{j=1}^{N-1} b_j T_j(s(x)) \right] \tag{B2}$$

with

$$s(x) \equiv \frac{\log_{10}(x/\Lambda\epsilon)}{\log_{10}(\Lambda/\epsilon)}, \tag{B3}$$

and where Λ is the ultraviolet cutoff, and ϵ is the infrared cutoff, only needed for numerical purposes. We require both integral equations to be satisfied at N fixed external momenta, in order to determine the $2N$ Chebyshev coefficients a_i, b_i. Using smooth expansions has the advantage of allowing us an absolute freedom in the choice of quadrature rules used to compute the various integrals numerically. This is required if we want to achieve a high accuracy in our results. The integration region is first split into an analytical integral over $[0,\epsilon^2]$ and a numerical integral over $[\epsilon^2,\Lambda^2]$. The integral over $[0,\epsilon^2]$ is computed analytically from the asymptotic infrared behavior discussed in Sec. V. This is needed as the infrared part of the integral is highly non-negligible, especially in the case of the gluon equation. For an efficient choice of quadrature rule we split the numerical integral into three regions, these are $[\epsilon^2,\min(x,\sigma)]$, $[\min(x,\sigma),\max(x,\sigma)]$ and $[\max(x,\sigma),\Lambda^2]$, where x is the external momentum and σ is the subtraction point. The splitting of the region of numerical integration into three subregions is needed as the integrands are not smooth at the boundaries of these regions and too much accuracy is lost if one uses quadrature rules spanning these boundaries. A sensible choice of quadrature rule on each integration region is for instance a composite 4-points Gaussian integration rule, where the composite rules are delimited by the region boundaries and the values of the external momenta at which we require the integral equation to be satisfied. This setup will yield $2N$ coupled, non-linear, algebraic equations for the $2N$ Chebyshev coefficients a_j and b_j. In traditional Dyson-Schwinger studies, the unknowns are usually determined by what is often called the *natural iteration method*, where the current approximation to the unknowns is used in the integrals of the right-hand side of the equations in order to provide a new approximation to the unknowns used in the left-hand side of the equations. This iteration method however is not necessarily convergent, and when it is convergent it often converges very slowly, as has been shown in Ref. [12]. This slow rate of convergence is not only inefficient, but more importantly it makes it very difficult to get a reliable estimate of the accuracy of the solution. For this reason, our numerical method uses the Newton method to solve sets of non-linear equations. This method uses the derivatives of the equations with respect to the unknowns to speed up the convergence. If the starting guess to the unknown coefficients is close enough to the solution, the convergence rate is even quadratic. Let us symbolically rewrite the coupled functional equations as follows:

$$f(x)[F,G]=0$$

$$g(x)[F,G]=0,$$

where f and g are equivalent to the Eqs. (11), (12) and $x \in [0,\Lambda^2]$. For the numerical solution, we require this equation to be satisfied at the external momenta x_i, the functions F and G are expanded as Chebyshev polynomials with coefficients a_j and b_j, and the integrals are approximated by a suitable quadrature rule. The equations then become

$$\tilde{f}(x_i)[a_j,b_j]=0$$

$$\tilde{g}(x_i)[a_j,b_j]=0,$$

where $i,j=0...N-1$ and $\tilde{f}$ and $\tilde{g}$ are the numerical approximations to f and g when the integrals are replaced with quadrature rules.

The Newton method will yield successive approximations to the solutions, given by

$$a_j^{n+1}=a_j^n-\Delta a_j^{n+1}$$

$$b_j^{n+1}=b_j^n-\Delta b_j^{n+1},$$

and the $(n+1)$-th improvements Δa_j^{n+1}, Δb_j^{n+1} are given by the solutions of the $2N\times 2N$ set of linear equations

$$\frac{\delta\tilde{f}^n(x_i)}{\delta a_j}\Delta a_j^{n+1}+\frac{\delta\tilde{f}^n(x_i)}{\delta b_j}\Delta b_j^{n+1}=0$$

$$\frac{\delta\tilde{g}^n(x_i)}{\delta a_j}\Delta a_j^{n+1}+\frac{\delta\tilde{g}^n(x_i)}{\delta b_j}\Delta b_j^{n+1}=0,$$

where the equations are taken at the N external momenta x_i and each equation includes implicit summations over j.

The total accuracy depends on the combination of the accuracies of the Chebyshev expansion and of the quadrature rule and on the convergence criterion of the Newton iteration.

APPENDIX C: STARTING GUESS

The Newton method, which is at the core of our numerical method, is a quadratically convergent iterative method, if the initial approximations to the unknown functions are *sufficiently close* to the exact solutions. The meaning of sufficiently close depends however entirely on the kernel of the integral equation. We observed that for the coupled gluon-ghost equations, the starting guess must not be too remote from the exact solution, if the method is to converge. This is in contrast with previous work on chiral symmetry breaking in QED and on the Mandelstam approximation to the gluon propagator in QCD, where the method was extremely insensitive to the starting guess.

It turns out that in the case of the coupled gluon-ghost equations, the starting guesses have to be chosen fairly accurately, especially in the asymptotic regions. In practice, we used the analytic asymptotic solutions to build good enough starting guesses for the form factors.

We want to find the solution parametrized by the leading infrared gluon coefficient A [defined in Eq. (24)] and F_1 $=F(1)$. The leading order infrared ghost coefficient is computed from Eq. (36):

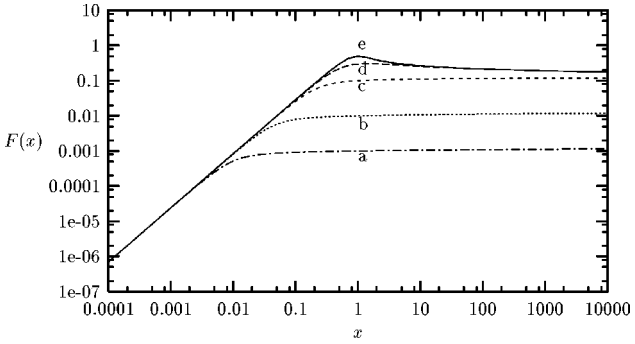

FIG. 6. Comparison of the solutions for $F(x)$ and $G(x)$ with their starting guesses used in the iterative Newton method, for $\lambda=1$, $A=1$ and $F_1=0.1$.

$$B=\sqrt{\frac{\nu}{\lambda\tilde{Z}_1 A}},$$

and we define $\tilde{x}$ as

$$\tilde{x}=\left(\frac{F_1}{A}\right)^{1/2\kappa},$$

which can be seen as a crude approximation to the bend-over point. A possible construction for the starting guesses is

$$F(x)=A\left[\frac{x}{\frac{x}{\tilde{x}}+1}\right]^{2\kappa}\left[4\nu\,\log\left(\frac{x}{\tilde{x}}+1\right)+1\right]^{1/8}$$

$$G(x)=B\left[\frac{x}{\frac{x}{\tilde{x}}+1}\right]^{-\kappa}\left[4\nu\,\log\left(\frac{x}{\tilde{x}}+1\right)+1\right]^{-9/16},$$

which has the correct leading infrared asymptotic behavior for $F(x)$ and $G(x)$ and agrees well with their leading ultraviolet logarithmic behavior, as is illustrated in Fig. 6.

Although it seems that the starting guesses $F(x)$ and $G(x)$ are extremely close to the final numerical solutions, we see that the Newton method does alter the running coupling $\alpha(x)=4\pi\lambda F(x)G^2(x)$ substantially while converging to the solution, as is shown in Fig. 7.

APPENDIX D: RUNGE-KUTTA METHOD

Rewrite the equations (11), (12), for $\sigma=1$, as

$$F^{-1}(x)=\eta+\lambda\left[\frac{G(x)}{x^2}\int_0^x dy\left(\frac{3y}{2}-\frac{y^2}{x}\right)G(y)+\int_x^1\frac{dy}{2y}G^2(y)\right] \tag{D1}$$

and

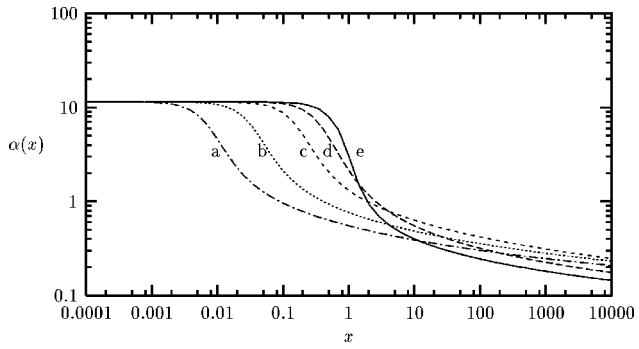

FIG. 7. Comparison of the solution for the running coupling $\alpha(x)$ with its starting guess, for $\lambda=1$, $A=1$ and $F_1=0.1$.

$$G^{-1}(x)=\zeta-\frac{9}{4}\lambda\left[\frac{F(x)}{x^2}\int_0^x dyyG(y)+\int_x^1\frac{dy}{y}F(y)G(y)\right], \tag{D2}$$

where η and ζ are constants. As discussed before we can choose $\lambda=1$, since an arbitrary value of λ can be recovered by applying an appropriate scaling to the form factors $F(x)$ and $G(x)$.

Let us rewrite the above equations in the form

$$F^{-1}(x)=\eta+\frac{3}{2}G(x)K(x)-G(x)L(x)+\frac{1}{2}\int_x^1\frac{dy}{y}G^2(y) \tag{D3}$$

and

$$G^{-1}(x)=\zeta-\frac{9}{4}F(x)K(x)-\frac{9}{4}\int_x^1\frac{dy}{y}F(y)G(y), \tag{D4}$$

where

$$K(x)=\frac{1}{x^2}\int_0^x dyyG(y) \tag{D5}$$

and

$$L(x)=\frac{1}{x^3}\int_0^x dyy^2G(y). \tag{D6}$$

On differentiating the above four equations, we obtain

$$\dot{F}=F^2[-\tfrac{3}{2}\dot{G}K-\tfrac{3}{2}G\dot{K}+\dot{G}L+G\dot{L}]+\tfrac{1}{2}F^2G^2$$

$$\dot{G}=\tfrac{9}{4}G^2[\dot{F}K+F\dot{K}]-\tfrac{9}{4}FG^3$$

$$\dot{K}=G-2K$$

$$\dot{L}=G-3L,$$

where $\dot{F}=dF/dt=x(dF/dx)$ etc., with $t=\log x$. After a little algebra, we can throw the first two of these equations into the form

$$\dot{F}=3F(X-Y)-FZ(\tfrac{3}{2}X-Y)$$

$$\dot{G}=ZG, \tag{D7}$$

where

$$X=FGK$$

$$Y=FGL$$

$$Z=\frac{X(3X-3Y-2)}{\frac{4}{9}+X(\frac{3}{2}X-Y)}. \tag{D8}$$

This system is suitable for an application of the Runge-Kutta method; but we must first address the question of the existence and multiplicity of the solutions, first of the differential system, and then of the integral equations (D3), (D4) from which they were derived. We already know an (exact) solution, namely

$$F(x)=Ax^{2\kappa}$$

$$G(x)=Bx^{-\kappa}, \tag{D9}$$

where κ was defined in Eq. (34), and where [compare Eq. (32) with $\lambda=1$]

$$B=\frac{2}{3\sqrt{A}}\left(\frac{1}{\kappa}-\frac{1}{2-\kappa}\right)^{-1/2}\approx\frac{0.955}{\sqrt{A}}. \tag{D10}$$

A priori we would expect there to be *four* free parameters for the differential system, corresponding say to the values of $F(1)$, $G(1)$, $K(1)$ and $L(1)$, from which the differential equations could step-by-step be integrated, for example by the Runge-Kutta method. In general, solutions of the differential system would not satisfy the requirements $x^2K(x)\to 0$ and $x^3L(x)\to 0$ as $x\to 0$. In fact the lower limits of the integrals in Eqs. (D5), (D6) would be incorrectly replaced by nonzero constants. Imposing the requisite boundary conditions at $x=0$, we expect to reduce the number of arbitrary constants in the general solution from four to two. Since there is a scaling invariance that leaves FG^2 unchanged, this means that, after we have removed this trivial degree of freedom by fixing A in Eq. (D9), we should still have one nontrivial free parameter. Where is it?

In Sec. VI we have seen that we can construct the following infrared asymptotic expansion, Eq. (50), for the general solutions $F(x)$ and $G(x)$:

$$F(x)=A_0x^{2\kappa}\left(1+\sum_{i=1}^{N}f_ia_1^ix^{i\rho}\right)$$

$$G(x)=B_0x^{-\kappa}\left(1+\sum_{i=1}^{N}g_ia_1^ix^{i\rho}\right). \tag{D11}$$

We expect these series to have zero radius of convergence, so they have been truncated in the anticipation that they are asymptotic series—that is, for small values of x, there will

be an optimal truncation point, N, for which the finite series is a good approximation. From this expansion we see that, besides the parameters A_0 and B_0, there is one more free parameter, a_1. On substituting the series for G in the definitions Eqs. (D5), (D6), we find

$$K(x)=B_0x^{-\kappa}\left(\frac{1}{-\kappa+2}+\sum_{i=1}^{N}\frac{g_ia_1^ix^{i\rho}}{-\kappa+i\rho+2}\right)$$

$$L(x)=B_0x^{-\kappa}\left(\frac{1}{-\kappa+3}+\sum_{i=1}^{N}\frac{g_ia_1^ix^{i\rho}}{-\kappa+i\rho+3}\right). \tag{D12}$$

The knowledge of the infrared asymptotic expansions for $F(x)$, $G(x)$, $K(x)$ and $L(x)$ allows us to use a Runge-Kutta method, starting from a momentum point deep in the infrared region and building the solution for increasing momenta. The Runge-Kutta method was run using the *NDSOLVE* routine of MATHEMATICA 3.0. The problem is solved as a function of $t=\log x$ and as the starting point, the IR series Eqs. (D11), (D12) are evaluated at $x=0.0001$ with $N=8$, using the coefficients f_j and g_j which are calculated with MATHEMATICA as well. The Runge-Kutta routine is run with 25 digit precision and 10,000 steps from $x=10^{-4}$ to $x=10^4$ for various values of $a_1<0$. The results produced by this method agree extremely well with those found with the direct integral equation method, as can be seen in Appendix E.

APPENDIX E: COMPARING THE RUNGE-KUTTA AND THE DIRECT METHOD

It is interesting to compare the two numerical methods used to solve the coupled set of integral equations. The Runge-Kutta method is a local method, which computes the function values at each point using the function values at neighboring points, starting from a momentum value deep in the infrared region and the asymptotic expansion at that point, while the direct integral equation method is a global method, the complete momentum range being solved simultaneously. Each method employs a different set of parameters. For a given λ, the Runge-Kutta method uses the infrared coefficients A_0 and a_1, while the direct method uses A_0 and F_1. To compare results, we first have to determine the parameter sets corresponding to the same solution in the three-dimensional space of solutions. We run the Runge-Kutta method with $\lambda=1$, $A_0=1$, and let a_1 vary till we find the solution yielding $F(1)=0.1$. As mentioned before this is found for $a_1=-10.27685$. We then compute the solutions of the Runge-Kutta method at the N values of external momenta used in the direct integral equation method and compare the numerical values found with both methods, using the maximum norm. For $N=81$, we find

$$\|F^{\rm dir}-F^{\rm RK}\|\equiv\max_{i=0}^{N-1}|F^{\rm dir}(x_i)-F^{\rm RK}(x_i)|=5.7\times10^{-5}$$

$$\|G^{\rm dir}-G^{\rm RK}\|\equiv\max_{i=0}^{N-1}|G^{\rm dir}(x_i)-G^{\rm RK}(x_i)|=6.0\times10^{-5}.$$

The agreement between these two very different numerical solution methods by far surpasses our initial expectations. Especially for the direct method it was hoped that the accuracy would be between 1/100 and 1/1000. However, the above mentioned numbers show that also this method achieves an even better accuracy.

The Newton iteration of the direct method requires about 4 iterations to converge and the program needs approximatively 19 sec real time to run on a Linux operated Pentium 200MHz PC. The Runge-Kutta method runs in approximatively 9 sec using the MATHEMATICA 3.0 routine NDSOLVE on the same computer. The use of two different methods is extremely important, to check the validity and accuracy of the solutions, especially in the case where the family of solutions is quite intricate.

Although the Runge-Kutta method is faster and very accurate, it can only be used if the integral equations can be transformed into differential equations+boundary conditions. It also requires a very accurate evaluation of the starting values of the functions using the infrared asymptotic expansion. When the problem cannot be turned into differential equations, only the direct method will be usable.

[1] G. 't Hooft, Nucl. Phys. **B33**, 173 (1971); **B35**, 167 (1971).

[2] H. D. Politzer, Phys. Rev. Lett. **30**, 1346 (1973).

[3] A useful overview can be found in C. D. Roberts and A. G. Williams, Prog. Part. Nucl. Phys. **33**, 477 (1994), and references contained therein.

[4] S. Mandelstam, Phys. Rev. D **20**, 3223 (1979).

[5] D. Atkinson, J. K. Drohm, P. W. Johnson, and K. Stam, J. Math. Phys. **22**, 2704 (1981); D. Atkinson, P. W. Johnson, and K. Stam, *ibid.* **23**, 1917 (1982).

[6] N. Brown and M. R. Pennington, Phys. Rev. D **38**, 2266 (1988); **39**, 2723 (1989); K. Büttner and M. R. Pennington, *ibid.* **52**, 5220 (1995).

[7] L. von Smekal, A. Hauck, and R. Alkofer, Phys. Rev. Lett. **79**, 3591 (1997); Ann. Phys. (N.Y.) **267**, 1 (1998).

[8] D. Atkinson and P. W. Johnson, Phys. Rev. D **37**, 2290 (1988); **37**, 2296 (1988); D. Atkinson, P. W. Johnson, and K. Stam, *ibid.* **37**, 2996 (1988).

[9] D. Atkinson and J. C. R. Bloch, Mod. Phys. Lett. A **13**, 1055 (1998).

[10] D. Atkinson, J. C. R. Bloch, and A. Hams (work in progress).

[11] J. C. Taylor, Nucl. Phys. **B33**, 436 (1971).

[12] J. C. R. Bloch, Ph.D. thesis, University of Durham, 1995; J. C. R. Bloch (in preparation).